Rnd3 is necessary for the correct oligodendrocyte differentiation and myelination in the central nervous system

Madrigal MP[1], Ballester-Lurbe B[1], Gómez O[2], Moreno-Bravo JA[3], Puelles E[3], Jurado S[3], Garcia-Verdugo JM[4], Pérez-Roger I[1], Terrado J[2]

[1] Departamento de Ciencias Biomédicas, Facultad de Ciencias de la Salud, Universidad CEU Cardenal Herrera, CEU Universities, Alfara del Patriarca, Valencia, Spain
[2] Departamento de Medicina y Cirugía Animal, Facultad de Veterinaria, Universidad CEU Cardenal Herrera, CEU Universities, Alfara del Patriarca, Valencia Spain
[3] Instituto de Neurociencias CSIC-UMH, San Juan de Alicante, Spain
[4] Laboratorio de Neurobiologia Comparada, Instituto Cavanilles de Biodiversidad y Biologia Evolutiva, Universidad de Valencia and CIBER de Enfermedades Neurodegenerativas (CIBERNED), Valencia, Spain

Corresponding author: José Terrado
e-mail address jterrado@uchceu.es
Orcid: 0000-0002-7356-2341

Declarations:

Funding: This work was supported by MINECO SAF2013-49176-C2-1-R, GV/2019/119, Conselleria de Innovación, Universidades, Ciencia y Sociedad digital and Programa Santander-FUSP. JAM-B is supported by the Ramón y Cajal Program (RYC2018-023868-I) from the Spanish Ministry of Science and Innovation.

Conflict of interest: Authors have no conflict of interest to declare.

Availability of data and material: The datasets generated during and/or analysed during the current study are available from the corresponding author on reasonable request.

Code availability: NA

Acknowledgment

This version of the article has been accepted for publication, after peer review but is not the Version of Record and does not reflect post-acceptance improvements, or any corrections. The Version of Record is available online at: http://dx.doi.org/10.1007/s00429-021-02419-0. Use of this Accepted Version is subject to the publisher's Accepted Manuscript terms of use https://www.springernature.com/gp/open-research/policies/acceptedmanuscript-terms

Abstract

Rho small GTPases are proteins with key roles in the development of the central nervous system. Rnd proteins are a subfamily of Rho GTPases characterized by their constitutive activity. Rnd3/RhoE is a member of this subfamily ubiquitously expressed in the CNS, whose specific functions during brain development are still not well defined. Since other Rho proteins have been linked to the myelination process, we study here the expression and function of Rnd3 in oligodendrocyte development. We have found that Rnd3 is expressed in a subset of oligodendrocyte precursor cells and of mature oligodendrocytes both *in vivo* and *in vitro.* We have analyzed the role of Rnd3 in myelination using mice lacking Rnd3 expression ($Rnd3^{gt/gt}$ mice), showing that these mice exhibit hypomyelination in the brain and a reduction in the number of mature and total oligodendrocytes in the corpus callosum and striatum. The mutants display a decreased expression of several myelin proteins and a reduction in the number of myelinated axons. In addition, myelinated axons exhibit thinner myelin sheaths. *In vitro* experiments using $Rnd3^{gt/gt}$ mutant mice showed that the differentiation of the precursor cells is altered in the absence of Rnd3 expression, suggesting that Rnd3 is directly required for the differentiation of oligodendrocytes and, in consequence, for the correct myelination of the CNS. This work shows Rnd3 as a new protein involved in oligodendrocyte maturation, opening new avenues to further study the function of Rnd3 in the development of the central nervous system and its possible involvement in demyelinating diseases.

Key words: Rnd3, GTPase, Myelin, Oligodendrocyte, Oligodendrocyte Precursor Cell.

Introduction

Oligodendrocytes (OLCs) are the myelin forming cells in the central nervous system (Nave and Werner 2014). OLCs are able to produce myelin and enwrap axons forming the myelin sheaths. Thereby, OLCs allow fast saltatory conduction of action potentials (Hartline and Colman 2007). Furthermore, myelin sheaths supply metabolic and trophic support to axons throughout their life (Fünfschilling et al. 2012; Nave and Trapp 2008) and contribute to neuroplasticity (McKenzie et al. 2014). Therefore, myelin is essential for the proper function of the nervous system, and its damage or deficit is associated with diseases such as multiple sclerosis (Nylander and Hafler 2012).

Oligodendrogenesis in the telencephalon is a complex and dynamic process during embryonic development. Progenitors along the neural tube give rise to oligodendrocyte precursor cells (OPCs) in three waves, from ventral to more dorsal regions, successively (Miller 2002; Qi et al. 2002; Yu et al. 1994). These three waves take place at different times along the embryonic development from E12.5 to the perinatal stage. Later, OPCs will migrate and develop into OLCs, populating the CNS (Kessaris et al. 2006; Miller 2002; Qi et al. 2002; Yu et al. 1994). In mice, myelination in the CNS starts at birth, peaks at P14-P15 and it is almost completed at two months of life in most brain regions (Vincze et al. 2008; Baumann and Pham-Dinh 2001).

Rnd3/RhoE (hereafter named Rnd3) is a member of the Rnd subfamily of Rho GTPases, whose main characteristic is the lack of GTPase activity, therefore being in a constitutively active state (Chardin 2006). Rnd3 is ubiquitously expressed in all regions of the adult brain and spinal cord, with the highest levels in the olfactory bulb and cortex (Ballester-Lurbe et al. 2009). Its expression peaks at the first 2–3 weeks of postnatal development and is gradually decreased as development approaches adulthood (Ballester-Lurbe et al. 2009). The main role of Rnd3 is to regulate the organization of the actin cytoskeleton in an antagonistic manner to RhoA, by inhibiting ROCK-I and activating p190RhoGAP (Guasch et al. 1998; Riento et al. 2003). Apart from the role in actin cytoskeleton organization, Rnd3 is involved in proliferation, by regulating cell cycle progression (Villalonga et al. 2004) and cellular transformation (Poch et al. 2007; Villalonga et al. 2004; Hernández-Sánchez et al. 2015). As a consequence, Rnd3 is involved in relevant functions in the nervous system. Previous results reveal the important role of Rnd3 in the normal development of the nervous system, such as the proper migration of cells along the Rostral Migratory Stream (RMS) and bulb olfactory cell development (Ballester-Lurbe et al. 2015). In addition, it has been reported that Rnd3 is involved in promoting cell migration (Guasch et al. 1998; Azzarelli et al. 2015) and in the polarity of neurons and glial cells (Peris et al. 2012). Related to these functions, there is evidence for the role of Rnd3 in cell differentiation (Liebig et al. 2009) . Finally, we have recently described that Rnd3 expression in corticospinal neurons is necessary for the formation of dendritic spines and extended axons and that Rnd3 maintains the radial glial scaffold at the striatopallidal junction that facilitates corticospinal axon pathfinding (Kaur et al. 2020). In addition, the absence of Rnd3 expression produces several defects in striatal and thalamocortical axonal projections as well as in the globus pallidus formation at early developmental stages (Marfull-Oromí et al. 2021).

To get insight into the *in vivo* function of Rnd3, null mice have been generated by our laboratory. Rnd3-null mice ($Rnd3^{gt/gt}$ mice) display important CNS disorders, such as hydrocephalus, an impaired performance in most neurobehavioral tests, a reduction in the number of spinal motor neurons, and a delay of neuromuscular maturation (Mocholí et al. 2011). Furthermore, Rnd3 deficient mice are smaller at birth, display growth delay and short lifespan. Finally, $Rnd3^{gt/gt}$ mice lack the common peroneal nerve and, consequently, show a complete

atrophy of its target muscles (Mocholí et al. 2011). At the molecular level, Rnd3$^{gt/gt}$ mice show an increased activity of both RhoA and ROCK, as well as in the LIMK-Cofilin pathway in brain (Peris et al. 2012).

We study here the role of Rnd3 in CNS myelination by using Rnd3$^{gt/gt}$ mice. Our results show that brains from mice lacking Rnd3 expression have a reduced level of myelin. We also show for the first time the expression of Rnd3 in OLCs and OPCs and demonstrate that Rnd3 is essential for the correct differentiation of OLCs. Together, our findings support a new role for Rnd3 during OLCs differentiation and, as a consequence, for the accurate myelination in CNS.

Results

Rnd3$^{gt/gt}$ mouse brains show a reduction in the amount of myelin

In order to study whether lack of Rnd3 expression could have an effect on the different brain cell populations, we analyzed P15 wild type (**Fig1. A, C, E, G**) and Rnd3$^{gt/gt}$ (**Fig.1 B, D, F, H**) mice brain sections by immunohistochemistry (IHC), using markers for neurons (NeuN, **Fig. 1C-D**), astrocytes (glial fibrillary acidic protein, GFAP, **Fig. 1E-F**) and oligodendrocytes (myelin basic protein, MBP, **Fig. 1G-H**). This analysis showed an apparent reduction of MBP labelling in the striatum and corpus callosum in mutant mice compared to wild types. Similar results were found with anti-MOG and anti-PLP antibodies (data not shown).

We then analyzed the expression of the same markers in protein extracts from the Striatum. The result shown in **Fig. 1I-J** reveals that the expression of NeuN and GFAP is the same in mutant than in wild type mice. However, there is a 50 % reduction in the expression of MBP in Rnd3 mutant mice compared to wild types.

Coronal sections of Rnd3$^{gt/gt}$ mice showed that the precise organization of the St was disturbed, showing a clear spatial disorganization (**Fig. 1K-M**). In wild type (**Fig. 1K**) and heterozygous (**Fig. 1L**) mice, a regular organization of groups of axons through the St was observed; however, in Rnd3$^{gt/gt}$ brain sections the density of the staining was clearly lower than in wt brain sections and the regular distribution of axons was lost (**Fig. 1M**). Also, the CC was evidently thinner in Rnd3$^{gt/gt}$ mice than in Rnd3$^{+/+}$ and Rnd3$^{+/gt}$ mice (**Fig. 1N-P**).

These results indicate that lack of Rnd3 expression affects mainly oligodendrocytes, but not neurons or astrocytes.

Rnd3 is expressed in oligodendrocyte precursor cells and in mature oligodendrocytes

We then studied the expression of Rnd3 in oligodendrocytes. Since Rnd3$^{+/gt}$ mice have the *β*-galactosidase (*βgal*) gene under control of the Rnd3 promoter, we used *βgal* as a reporter for Rnd3 expression. Using this strategy, the striatum (St) and the corpus callosum (CC) from P15 Rnd3$^{+/gt}$ mice were stained against *βgal* and Sox10 as a marker of the oligodendrocyte lineage. The Sox10 immunostaining was used to quantify the total number of OLCs, since it is expressed in OPCs and continues to be expressed in mature OLCs (Kuhlbrodt et al. 1998). Co-expression of *βgal* and Sox10 was only observed in a subset of Sox10 positive cells in both regions (arrowheads in **Fig. 2 A, D**). Likewise, not all *βgal* positive cells expressed Sox10. These results indicate that Rnd3 is expressed in a particular subtype of OLCs but that it is not a specific marker for this lineage, since *βgal* positive/Sox10 negative cells were also observed. We also used specific markers for OPCs (PDGFRa) or for mature OLCs (APC) (Bin et al. 2016), along with *βgal*. Our results showed that Rnd3 is

expressed in a subset of both, precursor and mature oligodendrocytes in the CC and the St (**Fig. 2B-C** and **2E-F**, respectively). Therefore, Rnd3 is expressed in a subset of cells all along the development of the OLC lineage.

The absence of Rnd3 alters the organization of myelin sheaths

To determine whether myelin organization was compromised in Rnd3$^{gt/gt}$ mice, coronal sections of CC and St from P15 wt and Rnd3$^{gt/gt}$ mice were analyzed by electron microscopy (EM). The CC of wt mice presented easily identifiable mature OLCs (**Fig. 3A**), whereas a high number of OLCs in an immature stage were observed in Rnd3$^{gt/gt}$ mice (**Fig. 3E**), suggesting a delay in OLCs maturation in the absence of Rnd3 expression. Electron micrographs from the myelinated region in the CC showed an apparent hypomyelination of axons in Rnd3$^{gt/gt}$ mice compared to controls, mainly because of a reduction in the myelin thickness, as well as in the number of myelinated axons in the mutants (**Fig. 3B** and **3F**). Altogether, this suggests an inefficient myelination process in the absence of Rnd3 expression. Finally, a detailed analysis of transverse axons showed that, while the myelin compaction was nearly complete in wt mice at P15 (**Fig. 3C**), myelin was defectively packed in most of the analyzed regions in Rnd3$^{gt/gt}$ brains (**Fig. 3G**). Strikingly, most myelinated fibers in the mutants showed oligodendroglial cytoplasm between the compacted lamellas and between the axon and the internal myelin layer (**Fig. 3G**). These results strongly support the idea that there is a delay in the myelination in the CC in the absence of Rnd3 expression. Ultrastructural analysis of the St also showed variations in the thickness of the myelin sheath and in the number of myelinated axons between wt and mutant mice (**Fig. 3I-J** and **3M-N**). As in the CC, immature forms of OLCs appeared to be more abundant in mutant than in wt mice (**Fig. 3M** and **3I**, respectively) and the myelin sheaths were thinner (**Fig. 3N** and **3J**, respectively).

To characterize in more detail these myelination defects in Rnd3$^{gt/gt}$ mice, the ratio between myelinated axons and total number of axons was quantified. In both, the CC and the St, the percentage of myelinated axons was significantly lower ($p<0.01$) in mutant compared to wt animals (73.51 % and 43.29 % reduction in CC and St, respectively, **Fig. 3D** and **3K)**. Next, since the EM results suggested a reduction or delay in the myelination process, the *g*-ratio was evaluated in the CC and St, in both Rnd3$^{gt/gt}$ and wt mice. At equal axonal diameter, high *g*-ratio indicates a relatively thinner myelin sheath (**Fig. 3L**). Indeed, Rnd3$^{gt/gt}$ mice presented higher *g*-ratio values both in the CC and St (**Fig. 3H** and **3O**), indicating a significantly thinner myelin sheath than control mice ($p<0.01$).

Rnd3$^{gt/gt}$ mice have a reduced number of mature oligodendrocytes in the Corpus Callosum and the Striatum

The reduced amount of myelin observed in Rnd3$^{gt/gt}$ mice might be the result of a reduction in the number of OLCs. To investigate this possibility, the number of OPCs and mature OLCs was quantified in the regions of interest in wt and mutant mice.

Oligodendrocytes at different stages of differentiation were analyzed in CC and St of wt and mutant P15 mice by using Sox10, as a marker of total OLCs, and PDGFRa, as a specific OPCs marker. These markers allowed us to distinguish between OPCs (Sox10+/PDGFRa+ cells) and mature OLCs (Sox10+/PDGFRa- cells; **Fig. 4A-H**). The different cell populations were counted, and the two genotypes were analyzed by a two-way

ANOVA (**Fig. 4I-J**). The result of the analysis shows that the oligodendrocyte populations in Rnd3$^{gt/gt}$ mice are different from the wt controls ($p=0.0196$ in the CC and $p<0.0001$ in the St), with a 19% decrease of the number of Sox10+ cells in the CC (**Fig. 4I**) and a 39% decrease in the St (**Fig. 4J**) of mutant mice compared to wt controls. There is also a significant decrease in the number of mature OLCs, counted as Sox10+/PDGFRa- cells ($p=0.0083$ in the CC and $p=0.0010$ in the St in a Bonferroni´s test). In fact, the percentage of mature OLCs in the CC is 68% in Rnd3$^{+/+}$ and 46% in Rnd3$^{gt/gt}$ mice, and in the St these values go down from 64% in wt to 48% in mutant mice, when compared to the total number of Sox10+ cells (**Fig. 4K-L**). These results suggest that lack of Rnd3 protein expression leads to a delay in the differentiation of OPCs into OLCs in the brain, with a concomitant defect in myelin production.

Lack of Rnd3 expression produces defects in oligodendrocyte differentiation *in vitro*

Rnd3 is expressed not only in OLCs but also in astrocytes and neurons (Peris et al., 2012; Guasch et al., 1998; Kaur et al., 2020). Therefore, the defects we have described could be due to the lack of Rnd3 expression in the OLCs (cell autonomous) or, on the contrary, as a result of defects in other cell populations, like astrocytes or neurons. We used an *in vitro* approach using OPCs in culture to determine whether the effect of the absence of Rnd3 expression on OLCs differentiation was cell autonomous. Cells from P0-P2 newborn forebrains were cultured on poly-L-lysine coated culture dishes. The differentiation process was induced by culturing cells in the presence of mitogens (PDGF-AA and FGF2) for one week to increase the number of OPCs, and in the absence of these mitogens for another week, resulting in a majority of mature OLCs (see material and methods section, Yang et al., 2005; Lee et al., 2007; Morello et al., 2011). The expression of Rnd3 (*β*gal positive cells) was analyzed at each stage of OLCs maturation in culture by performing immunocytochemistry (ICC) using anti-Sox10, anti-PDGFRa and anti-APC antibodies (**Fig. 5**). A subset of cells of the OLCs lineage (Sox10 positive) showed *β*gal labeling, indicative of Rnd3 expression (**Fig. 5A-A''**). There was *β*gal labeling also in a subpopulation of PDGFRa positive OPCs (**Fig. 5B-B''**) and in a subgroup of mature APC positive OLCs (**Fig. 5C-C''**).

Therefore, Rnd3 is expressed at all stages along the differentiation of the OLCs lineage and during the transition from OPCs to OLCs in culture, indicating that the *in vitro* approximation reproduces the *in vivo* process of OLCs differentiation. Undifferentiated cultures showed that most Sox10-IR cells were positive for PDGFRa, both in control and Rnd3$^{gt/gt}$ cultures (**Fig. 6A-C** and **6D-F**). As the cells begin to differentiate, APC positive cells started to appear both in Rnd3$^{+/+}$ and Rnd3$^{gt/gt}$ cultures (**Fig. 6G-I** and **6J-L)**. At the end of the differentiation protocol, we counted the total number of OLCs (Sox10+ cells), the number of immature OPCs (Sox10+/APC- cells) and the number of fully differentiated OLCs (Sox10+/APC+ cells). The distribution of the cell populations is significantly different between wt and mutant cultures ($p<0.0001$ in a two-way ANOVA), with an increase in the number of OPC, from 9.22 ± 1.94 cells per field of view (FOV) in wt to 22.07 ± 0.97 in the mutant cultures ($p<0.0001$ in a Bonferroni´s test, **Fig. 6M**). When compared to the total number of Sox10+ cells in each FOV, the percentage of mature OLCs is reduced from 48% in WT to 25% in Rnd3$^{gt/gt}$ cultures (**Fig. 6N**), indicating that the results obtained with cell cultures reproduce the observations in brain tissue, where the absence of Rnd3 expression results in a delay of oligodendrocyte differentiation.

All these data suggest, that Rnd3 expression is necessary for proper OLCs differentiation in a cell autonomous way and its absence could explain the alterations in myelin sheath formation observed in mice lacking Rnd3

expression. Therefore, Rnd3 is implicated in OLCs differentiation and thereby it is essential for their function in the CNS.

Discussion

In this work we have shown that Rnd3 is expressed all along the differentiation process of OLCs and that in its absence there is a defective maturation of OLCs. Subsequently, the total amount of the myelin related protein MBP is reduced in brain of mice lacking Rnd3 expression and there is a decrease in the number of myelinated axons, which, in addition, display a thinner myelin sheath. Altogether, these results indicate a new role for Rnd3 in the myelination process in the CNS.

Several Rho GTPases have been shown to be involved in the CNS myelination (Feltri et al. 2008; Thurnherr et al. 2006; Wolf et al. 2001). The expression and activity of Cdc42 and Rac1 increases as OLCs differentiation proceeds, and it seems that these proteins act as positive regulators of morphological differentiation, inducing process extension and branching (Liang et al. 2004). Conversely, RhoA is expressed and active during the early progenitor stages. *In vitro* experiments have demonstrated that the expression of constitutively active RhoA prevents OLCs process extension (Wolf et al. 2001), suggesting that RhoA may be a negative regulator of OLCs maturation, inhibiting process extension (Liang et al. 2004).

Different mechanisms affected by Rnd3, ranging from cell cycle to cytoskeletal dynamics control, can be involved in an aberrant OLCs development. Therefore, the lack of Rnd3 expression in Rnd3$^{gt/gt}$ mice in these regions at embryonic stages could be related to the defects observed in OPCs development. Indeed, the reduction of total OLCs in Rnd3$^{gt/gt}$ brains could be originated by a failure in OPCs cell proliferation control. Rnd3 overexpression blocks cell proliferation in several different models by affecting the cyclin D1 pathway of cell cycle regulation (Villalonga et al. 2004; Poch et al. 2007). Furthermore, fibroblasts derived from Rnd3$^{gt/gt}$ embryos show a higher proliferation rate and a lack of cell contact inhibition (Hernández-Sánchez et al. 2015) and in Rnd3$^{gt/gt}$ brains there is an increased cell proliferation at the SVZ compared to wt (Ballester-Lurbe et al. 2015). However, we have not found a higher number of Sox10 positive cells (including both OPCs and OLCs) in CC or in St, suggesting that there is no increase in the proliferation rate of these cells in the absence of Rnd3 expression.

Apoptosis could also explain the lower number of oligodendrocytes and the defects in myelination found in the absence of Rnd3 expression, as it has been reported that apoptosis induction in OLCs inhibits myelination (Caprariello et al. 2015). Although we have not analyzed apoptosis directly, it seems unlikely to be involved in our observations, as it has been shown that Rnd3 induces apoptosis and its deletion suppresses apoptosis in mouse brain (Dong et al. 2021), even though this was shown in mice slightly younger than ours (P7 vs P15). Therefore, further studies will be necessary to determine the mechanisms by which lack of Rnd3 cause these alterations.

It is generally accepted that astrocytes and neurons support OLC function by the release of external signals in order to facilitate each step of myelination: OPCs proliferation, differentiation and, finally, myelination (Domingues et al. 2016). Thus, it could be discussed whether the alterations observed in this work concerning OPCs *in vitro* and *in vivo* differentiation in the absence of Rnd3 could be produced by intrinsic defects of OPCs or induced by anomalies in cells of other lineages. *In vitro* experiments show that Rnd3$^{gt/gt}$ OPCs still

have problems in their differentiation, independently from external signals, since less OPCs differentiate to OLCs after stimulation in Rnd3$^{gt/gt}$ cultures compared to wt. These results suggest that the defect found during OPCs differentiation *in vivo* is endogenous and, therefore, Rnd3 plays a cell autonomous function for the differentiation of the OLCs.

Overexpression of a dominant negative RhoA mutant causes hyperextension of oligodendrocyte processes (Wolf et al. 2001) and a reduction of active RhoA has been shown to be necessary for OLCs differentiation (Liang et al. 2004). In addition, inhibition of RhoA expression through siRNA in OPCs triggers OPCs differentiation (Baer et al. 2009). Rnd3 has an opposing role to that of RhoA by at least two known mechanisms: activation of p190RhoGAP and inhibition of ROCK-I. Therefore, the lack of Rnd3 expression results in an increase of active RhoA protein. In fact, our previous results have shown that Rnd3$^{gt/gt}$ mice show a reduced expression of p190RhoGAP and increased active RhoA and ROCK in brains (Peris et al. 2012). Consequently, the absence of Rnd3 expression would result in an increase of the RhoA pathway activity leading to a decrease of OPCs differentiation. Hence, the results shown here suggest that Rnd3 can positively modulate OLCs differentiation by inhibiting the RhoA pathway and that Rnd3 expression is necessary for proper differentiation of OLCs.

Interestingly, a similar effect for Rnd2, another member of the Rnd subfamily, has been very recently shown (Miyamoto et al. 2021). Indeed, Rnd2 seems to have a positive effect on myelination in early postnatal animals, since the absence of Rnd2 in oligodendrocytes results in a decrease of myelin sheath formation. This could be explained in part by the activation of ROCK in Rnd2 knockout mice. However, Rnd2 seems to have an additional role since, at later periods, Rnd2 inhibits myelination, which has been suggested that could be done by breaking down excessively thick myelin membranes. At P28, Rnd2 expression is higher than at P14 and Rnd2 KO mice show a decrease in ROCK activity from P14 to P28 (Miyamoto et al. 2021).

We have not analyzed the role of Rnd3 in older animals. However, Rnd3 is expressed highly up to P21 and then its expression decreases (Ballester-Lurbe et al. 2009), whereas Rnd2 is barely detected before P14 and its expression is higher in adult mice (Miyamoto et al. 2021). In both cases, the absence of the expression of either Rnd protein at early postnatal stages (P15 in our case for Rnd3 and P14 in the case of the Rnd2 KO mice) results in an increased activity of the RhoA-ROCK pathway that, in turn, leads to a decreased myelination.

Therefore, both members of the Rnd subfamily have similar effects at least in young animals and in both cases it occurs in relation to the activation of ROCK. As such is the case, it is tempting to speculate that a delicate balance in the expression of the Rnd proteins, without being redundant, coordinately regulate the complex process of myelination.

Demyelination and defective myelination are in the basis of several devastating illnesses. Among them, Multiple Sclerosis is the most widespread (Nylander and Hafler 2012). It is not known whether Rho proteins, and more specifically Rnd3, can play a role in these diseases or whether they could be involved in hypothetic therapeutic approaches, but it is interesting to note that a role for Rho family of GTPases has been suggested in recovery of experimental autoimmune encephalomyelitis (EAE), a mouse model for Multiple Sclerosis. Indeed, lovastatin impedes demyelination and augments myelin repair in EAE through the inhibition of cholesterol biosynthesis (Paintlia et al. 2008). The activity of lovastatin in EAE is achieved, at least in part, through altering the activity of Rho GTPases in glial cells, since it induces the accumulation of RhoA, Cdc42 and Rac1 in the cytoplasm rather than in the membrane of OLCs. This seems to be produced through blocking

isoprenylation, causing then the accumulation of Rho proteins in the cytosol and its inactivation that, in turn, fails to activate ROCK downstream signaling (Paintlia et al. 2008). Moreover, statins have been shown to induce cell differentiation and OPCs process extension through RhoA inactivation (Miron et al. 2007). On the other hand, the treatment with matrine, a monomer that is used in traditional Chinese medicine as an anti-inflammatory agent, has beneficial effects in experimental EAE and significantly reduces the levels of NogoA, its receptor complex NgR/p75NTR/LINGO-1, and their downstream RhoA/ROCK signaling pathway in the CNS. In contrast, intracellular cyclic AMP (cAMP) levels and the cAMP dependent protein kinase (protein kinase A, PKA), which can promote axonal regrowth by inactivating RhoA, are upregulated (Kan et al. 2017).

As this work has unraveled a new role for Rnd3 in the maturation of the OLCs and myelination in the CNS, it opens new avenues for further studies into the molecular function of Rnd3 and its possible involvement in demyelinating diseases. However, more specific approaches are necessary to decipher the exact function of Rnd3 in the development of the CNS and the onset of these diseases.

Material and methods

Animal procedures

All animal procedures were approved by the local ethics committee (Ethics Committee for Animal Welfare of the Universidad CEU Cardenal Herrera, ID CEEA 16/023), met the national guidelines (Spanish law 53/2013) and the European regulations (EU directive 86/609). Mice deficient in Rnd3 expression ($Rnd3^{gt/gt}$) were generated by insertion of a gene-trap cassette in intron 2 of the gene, resulting in a mixed genetic background C57BL6/129S. The phenotype of these mice has been described previously (Mocholí et al. 2011). Mice were kept under controlled conditions of temperature (21 ± 1ºC), humidity (40-45%) and photoperiod (12h), having free access to water and food.

Western blotting

Mice were sacrificed by cervical dislocation. The western blot protocol used was similar to the previously described in publications from our group (Ballester-Lurbe et al. 2015). Mouse anti-NeuN (MAB377), anti-GFAP (MAB360), anti-MBP (ab7349), anti-Rnd3 (05-723) and anti-Actin (A-3854) primary antibodies were used with the corresponding secondary antibodies (goat anti-Mouse HRP; Pierce 31437) for the analysis of protein level expression in brains of mice lacking Rnd3 expression.

Histology and antibody staining

Mouse brains were fixed overnight in 4% paraformaldehyde in PBS. 5 μm paraffin sections were used with the following antibodies: mouse anti-NeuN (Millipore MAB377), mouse anti-GFAP (Millipore MAB360), mouse anti-ACP (Millipore OP80-100UG); chicken anti-β-galactosidase (Abcam ab936), goat anti-β-galactosidase (CAPPEL 56028), mouse anti-MBP (Abcam ab7349), rabbit anti-Neurofilament (Abcam ab64300), rabbit anti-PDGFRa (Santa Cruz sc-33), goat anti-Sox10 (R&D systems AF2864), mouse anti-Sox10 (Sigma SAB1402361). The secondary antibodies used were: ALEXA fluor 488 Goat anti-Chicken (Molecular Probes A 11039); ALEXA fluor 488 Donkey anti-Goat (Invitrogen A11055); ALEXA fluor 594 Donkey anti-Goat (Abcam ab150132); biotinylated Rabbit anti-Goat (Vector Laboratories BA-5000);

biotinlylated Donkey anti-Mouse (Abcam ab150108); ALEXA fluor 594 Goat anti-Mouse (Invitrogen A21207); ALEXA fluor 488 Goat anti-Mouse (Invitrogen A11029); biotinylated Goat anti-Mouse (Vector Laboratories BA-9200); ALEXA fluor 488 Donkey anti-Rabbit (Invitrogen A21206); ALEXA fluor 594 Donkey anti-Rabbit (Invitrogen A21207); biotinylated Goat anti-Rabbit (Vector Laboratories BA-1000).

The protocol for antibody staining of tissue sections was as previously described by (Ballester-Lurbe et al. 2015).

Electron microscopy

Brains from P15 mice ($Rnd3^{+/+}$ and $Rnd3^{gt/gt}$; three animals per genotype) were fixed O/N in a 2 % paraformaldehyde-2.5 % glutaraldehyde fixative solution and processed for electron microscopy as previously described (Ballester-Lurbe et al. 2015). Coronal sections were post-fixed in 2 % osmium tetroxide during 2 hours in the darkness. Samples were rinsed in H_2O, dehydrated in a series of increasing concentrations of ethanol and rinsed in propylene oxide (2x 10 min). Then, samples were transferred to araldite and they were incubated at 70° for 3 days in order to get the polymerization of the araldite. Semi-thin sections (1.5 µm) were mounted on gelatin-coated slides and stained with 1 % toluidine blue. Ultra-thin (60-70nm) sections were cut with a diamond knife, stained with lead citrate (Reynolds solution) and examined under a transmission electron microscope. Two telencephalon areas rich in myelinated axons were studied: corpus callosum (CC; from Bregma 1.10 to -0.10 mm) and dorsal striatum (St; from Bregma -1.28 to -1.64 mm).

Oligodendrocyte progenitor cells isolation and culture

For the isolation and culture of oligodendrocyte progenitor cells, we followed a previously described protocol (Cruz-Martinez et al. 2014). Briefly, brains from 3 neonate (P0-P2) mice were carefully removed, dissected and placed into a Petri dish. Then, samples were microdissected by chemical and physical tools and the resulting cellular suspension was placed on previously poly- L-lysine coated T-25 flasks. After one week, the obtained culture was mainly composed of astrocytes and a small amount of OPCs. In order to obtain a culture enriched in OLCs, the residual contaminating microglia and astrocytes were removed. Next, the culture medium was supplemented with mitogens (PDGF-AA and bFGF) to stimulate the proliferation of OPCs and 1 week later, these mitogens were removed to induce their differentiation into OLCs. Finally, OPCs and OLCs were analyzed by immunocytochemistry.

Immunocytochemistry

OPCs were cultured on poly-L-lysine coated coverslips. Cells were fixed for 10 min in 4 % paraformaldehyde and processed for Immunocytochemistry (ICC) following a standard protocol. Coverslips were rinsed 5 x 6 min in PBS and blocked with 3 % BSA, 0.1 % Triton and 10 % horse serum in PBS for 1 hour. They were then incubated O/N at 4 °C in blocking solution with the following primary antibodies: Mouse anti-APC (Millipore OP80-100UG), Goat anti-β-galactosidase (CAPPEL 56028), Rabbit anti-PDGFRa (Santa Cruz sc-338), Mouse anti-Sox10 (Sigma SAB1402361), Goat anti-Sox10 (R&D systems AF2864). Slides were washed in PBS for 30 min and incubated with the appropriate fluorescence labelled secondary antibodies 1hour at RT. DAPI was used to stain the nuclei.

Microscopy and quantification

Myelin quantification on brain sections. To determine the amount of myelin, the g-ratio was analyzed in different areas of $Rnd3^{+/+}$ and $Rnd3^{gt/gt}$ brains. The *g*-ratio refers to the ratio between axon diameter (d) and

fiber diameter (D), where fiber diameter includes the axon diameter and the thickness of the myelin sheath (Paus and Toro 2009). To quantify the *g*-ratio, 100 myelinated axons from non-overlapping electron micrographs were measured for each phenotype (n=3) at the CC (from Bregma 1.10 to -0.10 mm) and the St (from Bregma -1.28 to -1.64 mm). Micrographs were taken in random fields, using a transmission electron microscope (FEI Tecnai G2 Spirit BioTwin) and using a digital camera (Morada, Soft Imaging System, Olympus). The g-ratio was calculated as the ratio between the perimeter of the axons and the perimeter of the fiber using the ImageJ software.

*Microscopy and cell quantifications in brain slides***.** IHC staining on paraffin sections were visualized under automated DM6000B microscope (for wide-field) and MZ16FA Fluorescence Stereomicroscope (for fluorescence images). Images were acquired with a DFC350-FX (monochrome) or DC500 (color) digital cameras, using Leica Application Suite (LAS) AF6000 Software (version 2.0.2). Then, images were processed and assembled with Adobe Photoshop and Adobe Illustrator softwares.

For quantification of OLCs, the number of total OLCs (Sox10+ cells), OPCs (Sox10+/PDGFRa+ cells) and mature OLCs (Sox10+/PDGFRa- cells) in CC and St were counted. Immunostained brain 5 µm sections were analyzed from Bregma -1.28 to -1.64 mm. The number of OLCs was measured in a fixed volume of 200·300·5 μm^3 ($3 \cdot 10^5$ μm^3). Three animals per phenotype were analyzed.

Microscopy and cell quantifications in cell cultures. To quantify the number of OPCs and mature OLCs, average cell number per field of view (FOV) was calculated by counting the number of total OLCs (Sox10+ cells), OPCs (Sox10+/APC- cells) and mature OLCs (Sox10+/APC+ cells) in 9 random 20X fields per cell culture (n = 3). Quantifications were performed on micrographs taken using a confocal DM5500-Q and with the ImageJ software.

Statistical analysis

Results are presented as mean values +/- standard error of the mean. Microsoft Excel and GraphPad Prism were used for statistical analysis of the data. A standard Student's t test was used for comparing the mean values of the data sets. Two-way ANOVA and Bonferroni's multiple comparisons test were used to analyze differences in cell distributions between genotypes, both in tissue and in culture. Differences were considered statistically significant when the obtained p-value was lower than 0.05. *$p<0.05$, **$p<0.01$, ***$p<0.001$.

Figures legend

Figure 1. $Rnd3^{gt/gt}$ mice show altered myelin basic protein expression in brain. Paraffin P15 wt (A, C, E, G) and $Rnd3^{gt/gt}$ (B, D, F, H) mice coronal brain sections were analyzed by cresyl violet staining (A-B) and by IHC using antibodies against NeuN (C-D), GFAP (E-F) and MBP (G-H). NeuN, GFAP and MBP proteins expression was analyzed by western blotting using St samples from wt and mutant mice (I). Rnd3 expression was used as genotype control. Actin was used as loading control. WB quantification shows a significant reduction only in MBP levels in mutant mice when compared to wt (J). Detailed view of MBP immunolabelled st (K-M) and corpus callosum (N-P) of Rnd3 wt (K, N), $Rnd3^{+/gt}$ (L, O) and $Rnd3^{gt/gt}$ (M, P). CC: Corpus

Callosum; St: Striatum.

Figure 2. Rnd3 is expressed in OPCs and OLCs *in vivo*. Representative coronal sections of the CC (A-C) and the St (D-F) from P15 $Rnd3^{+/gt}$ mice were immunostained with anti-*βgal* antibodies (green) and different OLC markers: anti-Sox10 in A and D; anti-PDGFRa in B and E; anti-APC in C and F (red); and DAPI (blue). *βgal* is co-expressed with the three OLC markers in both regions (arrowheads). CC: Corpus Callosum; St: Striatum. Scale bar: 25 µm.

Figure 3. The absence of Rnd3 expression alters the organization of the myelin sheath in the CC and St. Representative electron micrographs of the CC in wt (A-C) and $Rnd3^{gt/gt}$ mice (E-G) at different magnifications. In wt animals, mature OLC (black arrowheads) were abundant (A), but in $RhoE^{gt/gt}$ brains the presence of more immature precursors (white arrowheads) was consistently detected (E). Myelinated axons show a higher myelin compaction in wt than in $Rnd3^{gt/gt}$ mice. C and G show the detail of the myelin compaction in wt and $Rnd3^{gt/gt}$ mice, respectively. Representative electron micrographs of the St in wt (I-J) and $Rnd3^{gt/gt}$ mice (M-N) at different magnifications. Black arrowheads indicate mature OLC and white arrowheads indicate immature OLC. The total number of myelinated axons and the myelin thickness are reduced in the CC and the St of $Rnd3^{gt/gt}$ mice. The percentage of myelinated axons in the CC and the St is lower in $Rnd3^{gt/gt}$ mice (D and K; p-value CC = 0.00004; St = 0.0019; n= 3 animals per genotype; 100 myelinated axons from non-overlapping electron micrographs were measured for each phenotype; unmyelinated axons were considered when their content was homogeneous and slightly electron dense with a round contour is round and lacking irregularities or lateral expansions.). The *g*-ratio analysis, represented schematically in L (adapted from Paus et al., 2009), shows a reduction in the myelin sheath of $Rnd3^{gt/gt}$ mice in a Student's *t* test, in both CC and St (H and O; p-value CC = 0.0061; St = 0.0156; n= 3 animals per genotype). Results are shown as the mean ± standard deviation. CC: Corpus Callosum; St: Striatum. Scale bar A, E, J, N= 5 µm; I, M = 10 µm; B, F = 1 µm; C, G = 100 nm.

Figure 4. Analysis of Sox10 and PDGFRa expression to identify OLC and OPC populations in wt and $Rnd3^{gt/gt}$ P15 mice. Brain coronal sections of the CC (A, B, E, F) and St (C, D, G, H) of wt (A-D) and Rnd3 mutant (E-H) mice were immunostained with antibodies against Sox10 (in green) and PDGFRa (in red). All cells of the OLC lineage are positive for Sox10 (red), OPCs are Sox10 and PDGFRa positive (yellow) and mature OLCs are Sox10 positive and PDRGFa negative (green). CC: Corpus Callosum; St: Striatum. Scale bar= 50 µm. Number of cells per volume in the CC (I) and in the St (J) showing that the oligodendrocyte populations in $Rnd3^{gt/gt}$ mice are different from the wt controls ($p=0.0196$ in the CC and $p<0.0001$ in the St). There is also a significant decrease in the number of mature OLCs, counted as Sox10+/PDGFRa- cells ($p=0.0083$ in the CC (I) and $p=0.0010$ in the St (J)). K and L show the percentage of OPCs and mature OLCs when compared to the total number of Sox10+ cells in the CC (K) and in the St (L).

Figure 5. Rnd3 is expressed during the differentiation process of OLCs *in vitro*. ICC of different OLC markers in the differentiation culture medium conditions showed Rnd3 expression (*βgal+*, green) in all differentiation stages: in A-A'', total OLC lineage (Sox10 positive); in B-B'', OPCs (PDGFRa positive); in C-C'', mature OLCs (APC positive). In all images, blue staining corresponds to the nuclei (DAPI). OPC: Oligodendrocyte Precursor Cells; OLC: Oligodendrocytes. Scale bar: 50 µm.

Figure 6. Rnd3 deficiency alters the differentiation of oligodendrocytes *in vitro*. Undifferentiated cultures showed that most Sox10-IR cells (green) were positive for PDGFRa (red), both in control and $Rnd3^{gt/gt}$ cultures

(A-C and D-F, respectively). Differentiated OLCs are Sox10+/APC/+ (G-L). Scale Bar A-F: 50 µm; G-L: 100 µm. In M, the number of Sox10+ (Total) Sox10+/APC- (OPCs), Sox10+/APC+ (OLCs) cells per field of view (FOV) at the end of the differentiation protocol is shown. Columns represent the mean value + SEM of cultures obtained from three different animals of each genotype. At least 9 different 20X FOV were counted from each culture. In N, the percentage of OPCs (Sox10+/APC-) and mature OLCs (Sox10+/APC+) when compared to the total number of Sox10+ cells is shown.

References

Azzarelli, R., F. Guillemot, and E. Pacary. 2015. Function and regulation of Rnd proteins in cortical projection neuron migration. *Front Neurosci* 9:19.

Baer, A. S., Y. A. Syed, S. U. Kang, D. Mitteregger, R. Vig, C. Ffrench-Constant, R. J. Franklin, F. Altmann, G. Lubec, and M. R. Kotter. 2009. Myelin-mediated inhibition of oligodendrocyte precursor differentiation can be overcome by pharmacological modulation of Fyn-RhoA and protein kinase C signalling. *Brain* 132 (Pt 2):465-481.

Ballester-Lurbe, B., S. González-Granero, E. Mocholí, E. Poch, M. García-Manzanares, M. Dierssen, I. Pérez-Roger, J. M. García-Verdugo, R. M. Guasch, and J. Terrado. 2015. RhoE deficiency alters postnatal subventricular zone development and the number of calbindin-expressing neurons in the olfactory bulb of mouse. *Brain Struct Funct* 220 (6):3113-3130.

Ballester-Lurbe, B., E. Poch, E. Mocholí, R. M. Guasch, I. Pérez-Roger, and J. Terrado. 2009. RhoE is spatiotemporally regulated in the postnatal mouse CNS. *Neuroscience* 163 (2):586-593.

Baumann, N., and D. Pham-Dinh. 2001. Biology of oligodendrocyte and myelin in the mammalian central nervous system. *Physiol Rev* 81 (2):871-927.

Bin, J. M., S. N. Harris, and T. E. Kennedy. 2016. The oligodendrocyte-specific antibody 'CC1' binds Quaking 7. *J Neurochem* 139 (2):181-186.

Caprariello, A. V., C. E. Batt, I. Zippe, R. R. Romito-DiGiacomo, M. Karl, and R. H. Miller. 2015. Apoptosis of Oligodendrocytes during Early Development Delays Myelination and Impairs Subsequent Responses to Demyelination. *J Neurosci* 35 (41):14031-14041.

Cruz-Martinez, P., A. Martinez-Ferre, J. Jaramillo-Merchán, A. Estirado, S. Martinez, and J. Jones. 2014. FGF8 activates proliferation and migration in mouse post-natal oligodendrocyte progenitor cells. *PLoS One* 9 (9):e108241.

Chardin, P. 2006. Function and regulation of Rnd proteins. *Nat Rev Mol Cell Biol* 7 (1):54-62.

Domingues, H. S., C. C. Portugal, R. Socodato, and J. B. Relvas. 2016. Corrigendum: Oligodendrocyte, Astrocyte and Microglia Crosstalk in Myelin Development, Damage, and Repair. *Front Cell Dev Biol* 4:79.

Dong, H., Q. Sun, Y. Zhang, Y. Li, F. Yuan, S. Mao, and B. Liu. 2021. Genetic deletion of Rnd3 suppresses apoptosis through NF-κB signaling in the brain. *Oncol Rep* 45 (2):595-605.

Feltri, M. L., U. Suter, and J. B. Relvas. 2008. The function of RhoGTPases in axon ensheathment and myelination. *Glia* 56 (14):1508-1517.

Fünfschilling, U., L. M. Supplie, D. Mahad, S. Boretius, A. S. Saab, J. Edgar, B. G. Brinkmann, C. M. Kassmann, I. D. Tzvetanova, W. Möbius, F. Diaz, D. Meijer, U. Suter, B. Hamprecht, M. W. Sereda, C. T. Moraes, J. Frahm, S. Goebbels, and K. A. Nave. 2012. Glycolytic oligodendrocytes maintain myelin and long-term axonal integrity. *Nature* 485 (7399):517-521.

Guasch, R. M., P. Scambler, G. E. Jones, and A. J. Ridley. 1998. RhoE regulates actin cytoskeleton organization and cell migration. *Mol Cell Biol* 18 (8):4761-4771.

Hartline, D. K., and D. R. Colman. 2007. Rapid conduction and the evolution of giant axons and myelinated fibers. *Curr Biol* 17 (1):R29-35.

Hernández-Sánchez, M., E. Poch, R. M. Guasch, J. Ortega, I. López-Almela, I. Palmero, and I. Pérez-Roger. 2015. RhoE is required for contact inhibition and negatively regulates tumor initiation and progression. *Oncotarget* 6 (19):17479-17490.

Kan, Q. C., H. J. Zhang, Y. Zhang, X. Li, Y. M. Xu, R. Thome, M. L. Zhang, N. Liu, Y. J. Chu, G. X. Zhang, and L. Zhu. 2017. Matrine Treatment Blocks NogoA-Induced Neural Inhibitory Signaling Pathway in Ongoing Experimental Autoimmune Encephalomyelitis. *Mol Neurobiol* 54 (10):8404-8418.

Kaur, N., W. Han, Z. Li, M. P. Madrigal, S. Shim, S. Pochareddy, F. O. Gulden, M. Li, X. Xu, X. Xing, Y. Takeo, Z. Li, K. Lu, Y. Imamura Kawasawa, B. Ballester-Lurbe, J. A. Moreno-Bravo, A. Chédotal, J. Terrado, I. Pérez-Roger, A. J. Koleske, and N. Sestan. 2020. Neural Stem Cells Direct Axon Guidance via Their Radial Fiber Scaffold. *Neuron* 107 (6):1197-1211.e1199.

Kessaris, N., M. Fogarty, P. Iannarelli, M. Grist, M. Wegner, and W. D. Richardson. 2006. Competing waves of oligodendrocytes in the forebrain and postnatal elimination of an embryonic lineage. *Nat Neurosci* 9 (2):173-179.

Kuhlbrodt, K., B. Herbarth, E. Sock, J. Enderich, I. Hermans-Borgmeyer, and M. Wegner. 1998. Cooperative function of POU proteins and SOX proteins in glial cells. *J Biol Chem* 273 (26):16050-16057.

Liang, X., N. A. Draghi, and M. D. Resh. 2004. Signaling from integrins to Fyn to Rho family GTPases regulates morphologic differentiation of oligodendrocytes. *J Neurosci* 24 (32):7140-7149.

Liebig, T., J. Erasmus, R. Kalaji, D. Davies, G. Loirand, A. Ridley, and V. M. Braga. 2009. RhoE Is required for keratinocyte differentiation and stratification. *Mol Biol Cell* 20 (1):452-463.

Marfull-Oromí, P., C. Fleitas, B. Zammou, D. Rocandio, B. Ballester-Lurbe, J. Terrado, I. Perez-Roger, C. Espinet, and J. Egea. 2021. Genetic ablation of the Rho GTPase Rnd3 triggers developmental defects in internal capsule and the globus pallidus formation. *J Neurochem* 158 (2):197-216.

McKenzie, I. A., D. Ohayon, H. Li, J. P. de Faria, B. Emery, K. Tohyama, and W. D. Richardson. 2014. Motor skill learning requires active central myelination. *Science* 346 (6207):318-322.

Miller, R. H. 2002. Regulation of oligodendrocyte development in the vertebrate CNS. *Prog Neurobiol* 67 (6):451-467.

Miron, V. E., S. Rajasekharan, A. A. Jarjour, S. S. Zamvil, T. E. Kennedy, and J. P. Antel. 2007. Simvastatin regulates oligodendroglial process dynamics and survival. *Glia* 55 (2):130-143.

Miyamoto, Y., T. Torii, M. Terao, S. Takada, A. Tanoue, H. Katoh, and J. Yamauchi. 2021. Rnd2 differentially regulates oligodendrocyte myelination at different developmental periods. *Mol Biol Cell* 32 (8):769-787.

Mocholí, E., B. Ballester-Lurbe, G. Arqué, E. Poch, B. Peris, C. Guerri, M. Dierssen, R. M. Guasch, J. Terrado, and I. Pérez-Roger. 2011. RhoE deficiency produces postnatal lethality, profound motor deficits and neurodevelopmental delay in mice. *PLoS One* 6 (4):e19236.

Nave, K. A., and B. D. Trapp. 2008. Axon-glial signaling and the glial support of axon function. *Annu Rev Neurosci* 31:535-561.

Nave, K. A., and H. B. Werner. 2014. Myelination of the nervous system: mechanisms and functions. *Annu Rev Cell Dev Biol* 30:503-533.

Nylander, A., and D. A. Hafler. 2012. Multiple sclerosis. *J Clin Invest* 122 (4):1180-1188.

Paintlia, A. S., M. K. Paintlia, A. K. Singh, and I. Singh. 2008. Inhibition of rho family functions by lovastatin promotes myelin repair in ameliorating experimental autoimmune encephalomyelitis. *Mol Pharmacol* 73 (5):1381-1393.

Paus, T., and R. Toro. 2009. Could Sex Differences in White Matter be Explained by g ratio? *Front Neuroanat* 3:14.

Peris, B., S. Gonzalez-Granero, B. Ballester-Lurbe, J. M. García-Verdugo, I. Pérez-Roger, C. Guerri, J. Terrado, and R. M. Guasch. 2012. Neuronal polarization is impaired in mice lacking RhoE expression. *J Neurochem* 121 (6):903-914.

Poch, E., R. Miñambres, E. Mocholí, C. Ivorra, A. Pérez-Aragó, C. Guerri, I. Pérez-Roger, and R. M. Guasch. 2007. RhoE interferes with Rb inactivation and regulates the proliferation and survival of the U87 human glioblastoma cell line. *Exp Cell Res* 313 (4):719-731.

Qi, Y., D. Stapp, and M. Qiu. 2002. Origin and molecular specification of oligodendrocytes in the telencephalon. *Trends Neurosci* 25 (5):223-225.

Riento, K., R. M. Guasch, R. Garg, B. Jin, and A. J. Ridley. 2003. RhoE binds to ROCK I and inhibits downstream signaling. *Mol Cell Biol* 23 (12):4219-4229.

Thurnherr, T., Y. Benninger, X. Wu, A. Chrostek, S. M. Krause, K. A. Nave, R. J. Franklin, C. Brakebusch, U. Suter, and J. B. Relvas. 2006. Cdc42 and Rac1 signaling are both required for and act synergistically in the correct formation of myelin sheaths in the CNS. *J Neurosci* 26 (40):10110-10119.

Villalonga, P., R. M. Guasch, K. Riento, and A. J. Ridley. 2004. RhoE inhibits cell cycle progression and Ras-induced transformation. *Mol Cell Biol* 24 (18):7829-7840.

Vincze, A., M. Mázló, L. Seress, S. Komoly, and H. Abrahám. 2008. A correlative light and electron microscopic study of postnatal myelination in the murine corpus callosum. *Int J Dev Neurosci* 26 (6):575-584.

Wolf, R. M., J. J. Wilkes, M. V. Chao, and M. D. Resh. 2001. Tyrosine phosphorylation of p190 RhoGAP by Fyn regulates oligodendrocyte differentiation. *J Neurobiol* 49 (1):62-78.

Yu, W. P., E. J. Collarini, N. P. Pringle, and W. D. Richardson. 1994. Embryonic expression of myelin genes: evidence for a focal source of oligodendrocyte precursors in the ventricular zone of the neural tube. *Neuron* 12 (6):1353-1362.

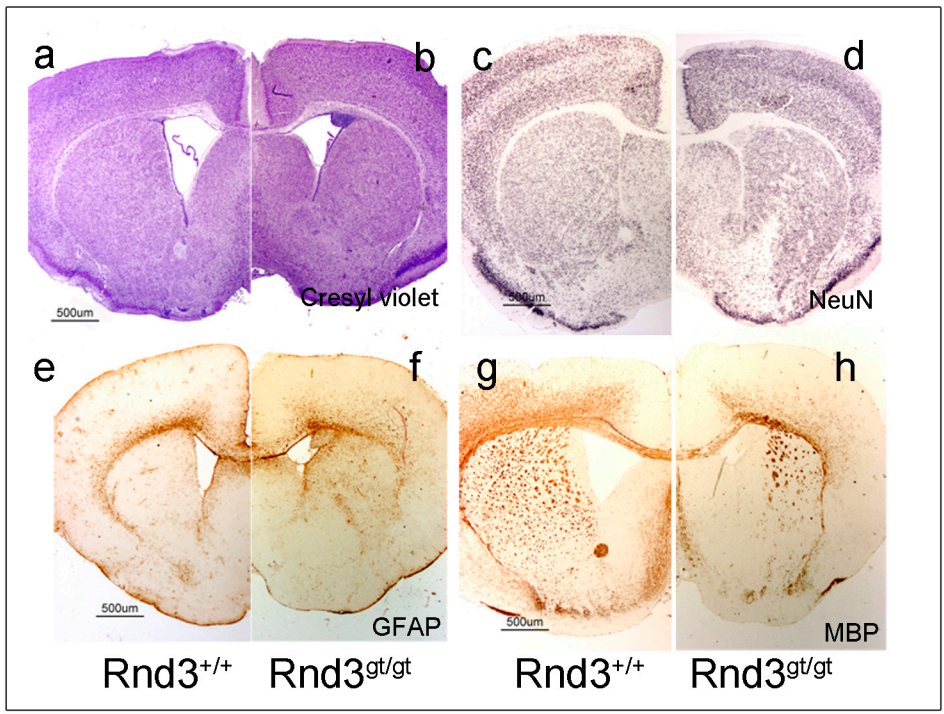
a
b
Cresyl violet
500um
c
d
NeuN
e
f
GFAP
500um
g
h
MBP
500um
Rnd3+/+
Rnd3gt/gt
Rnd3+/+
Rnd3gt/gt

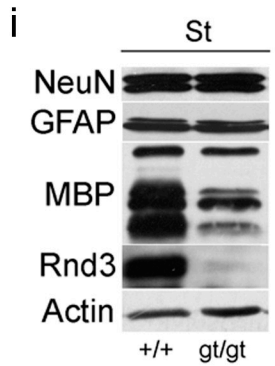
i
St
NeuN
GFAP
MBP
Rnd3
Actin
+/+
gt/gt

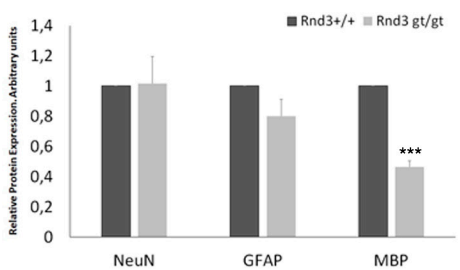
j
Rnd3+/+
Rnd3 gt/gt
Relative Protein Expression. Arbitrary units
1,4
1,2
1
0,8
0,6
0,4
0,2
0
***
NeuN
GFAP
MBP

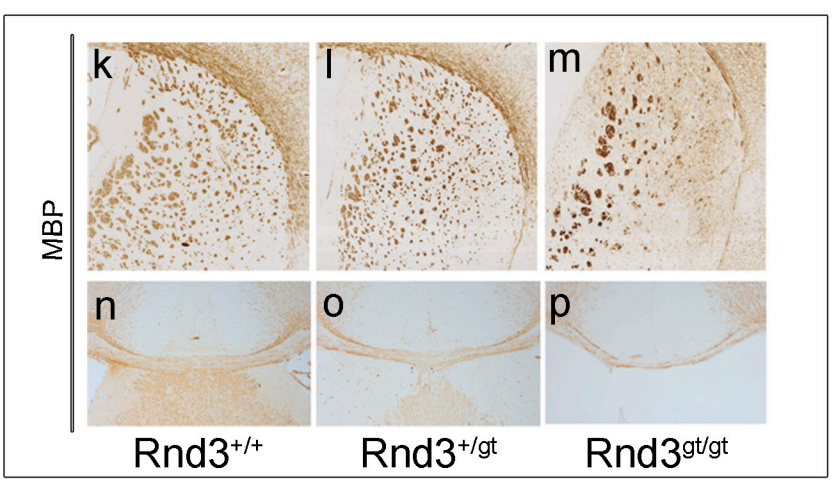
MBP
k
l
m
n
o
p
Rnd3+/+
Rnd3+/gt
Rnd3gt/gt

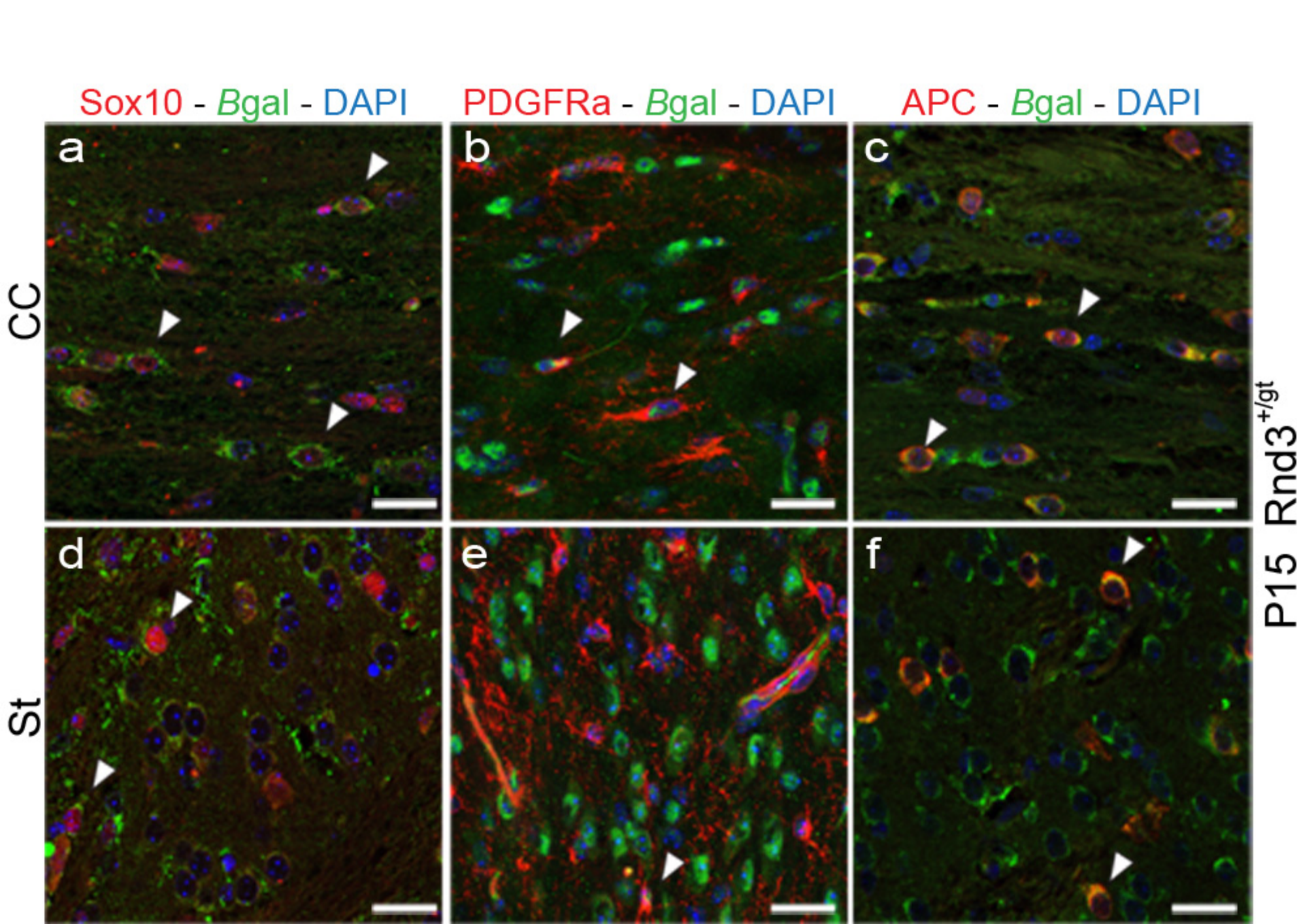
Sox10 - Bgal - DAPI
PDGFRa - Bgal - DAPI
APC - Bgal - DAPI
a
b
c
d
e
f
CC
St
P15 Rnd3+/gt

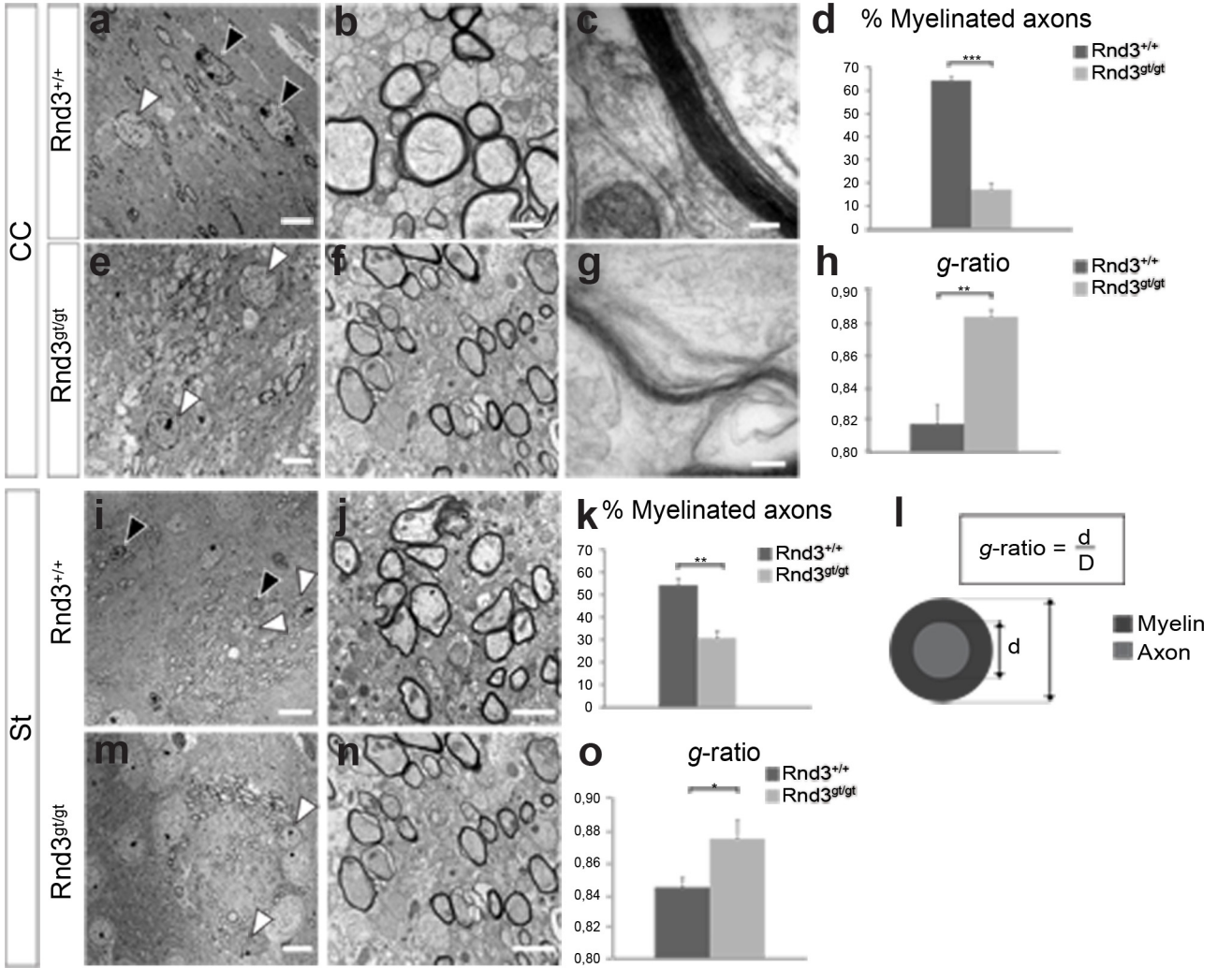
CC
St
Rnd3+/+
Rnd3gt/gt
a
b
c
d
% Myelinated axons
***
Rnd3+/+
Rnd3gt/gt
70
60
50
40
30
20
10
0
e
f
g
h
g-ratio
**
0,90
0,88
0,86
0,84
0,82
0,80
i
j
k
% Myelinated axons
**
l
g-ratio = d/D
d
Myelin
Axon
m
n
o
g-ratio
*

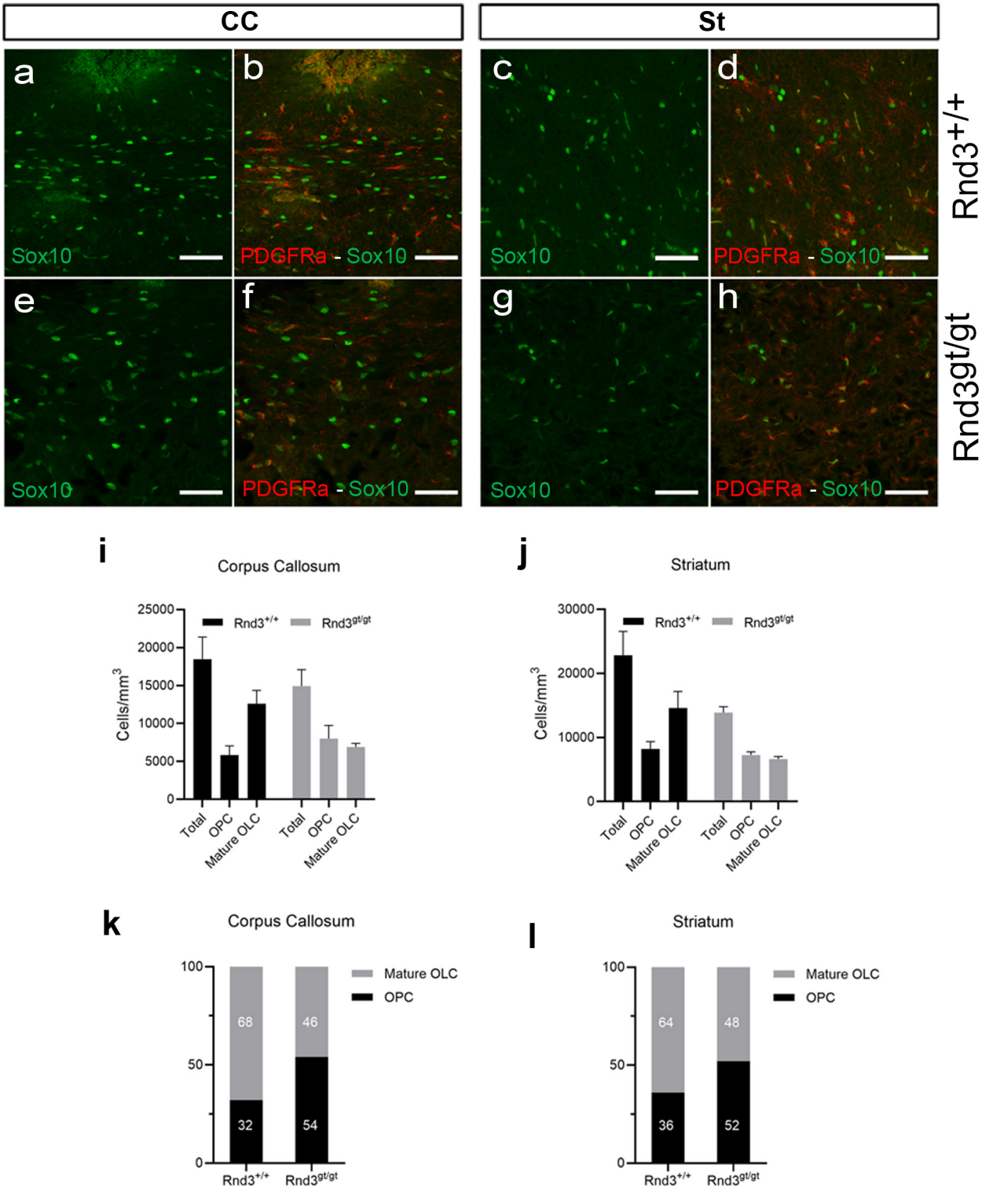
cc
St
a
b
c
d
e
f
g
h
Sox10
PDGFRa - Sox10
Rnd3+/+
Rnd3gt/gt
i
Corpus Callosum
Cells/mm3
Rnd3+/+
Rnd3gt/gt
Total
OPC
Mature OLC
j
Striatum
k
Corpus Callosum
Mature OLC
OPC
68
46
32
54
l
Striatum
64
48
36
52

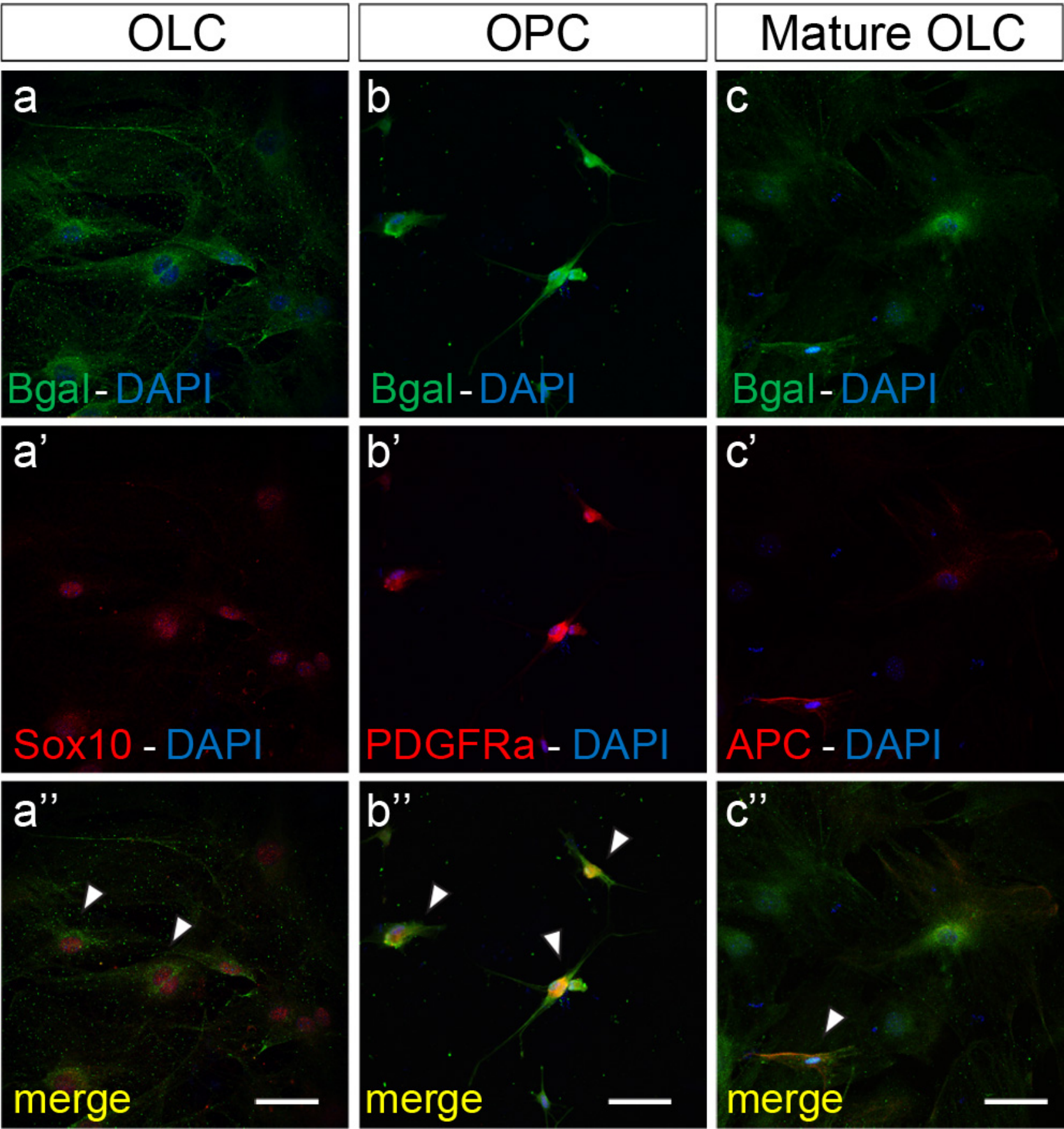
OLC
OPC
Mature OLC
a
b
c
Bgal - DAPI
Bgal - DAPI
Bgal - DAPI
a'
b'
c'
Sox10 - DAPI
PDGFRa - DAPI
APC - DAPI
a''
b''
c''
merge
merge
merge

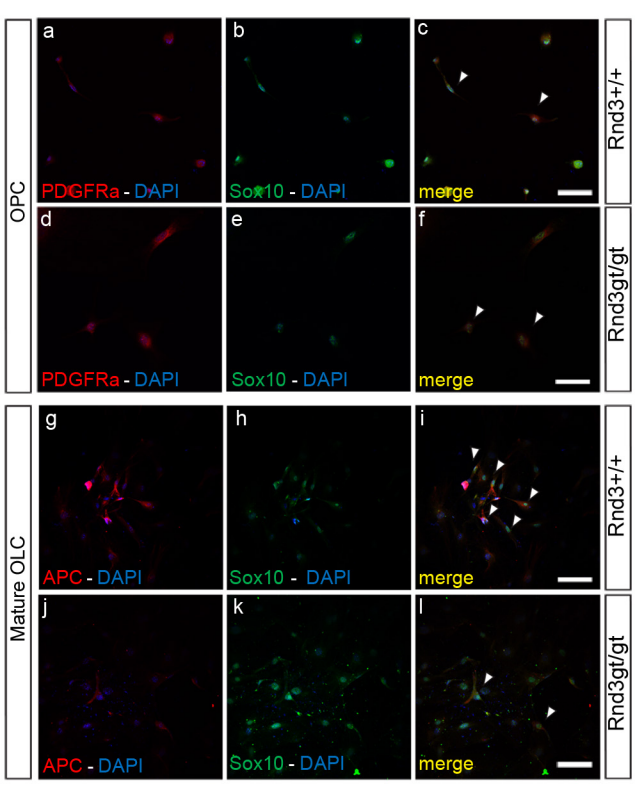
OPC
Mature OLC
a
b
c
d
e
f
g
h
i
j
k
l
PDGFRa - DAPI
Sox10 - DAPI
merge
APC - DAPI
Rnd3+/+
Rnd3gt/gt

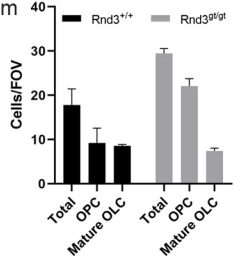
m
Rnd3+/+
Rnd3gt/gt
Cells/FOV
40
30
20
10
0
Total
OPC
Mature OLC

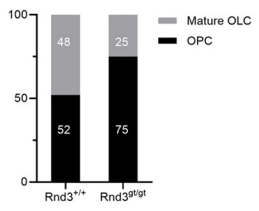
n
100
50
0
48
52
25
75
Mature OLC
OPC
Rnd3+/+
Rnd3gt/gt